The reduction of lipid-sourced energy production caused by ATGL inhibition cannot be compensated by activation of HSL, autophagy, and utilization of other nutrients in fish

Si-Lan Han, Yan Liu, Samwel M. Limbu, Li-Qiao Chen, Mei-Ling Zhang & Zhen-Yu Du



Fish Physiology and Biochemistry

ISSN 0920-1742

Fish Physiol Biochem
DOI 10.1007/s10695-020-00904-7

Springer

Your article is protected by copyright and all rights are held exclusively by Springer Nature B.V.. This e-offprint is for personal use only and shall not be self-archived in electronic repositories. If you wish to self-archive your article, please use the accepted manuscript version for posting on your own website. You may further deposit the accepted manuscript version in any repository, provided it is only made publicly available 12 months after official publication or later and provided acknowledgement is given to the original source of publication and a link is inserted to the published article on Springer's website. The link must be accompanied by the following text: "The final publication is available at link.springer.com".



Author's personal copy

Fish Physiol Biochem
https://doi.org/10.1007/s10695-020-00904-7

The reduction of lipid-sourced energy production caused by ATGL inhibition cannot be compensated by activation of HSL, autophagy, and utilization of other nutrients in fish

Si-Lan Han · Yan Liu · Samwel M. Limbu · Li-Qiao Chen · Mei-Ling Zhang · Zhen-Yu Du

Received: 16 July 2020 / Accepted: 18 November 2020
© Springer Nature B.V. 2020

Abstract The adipose triglyceride lipase (ATGL) and hormone-sensitive lipase (HSL)–mediated lipolysis play important roles in lipid catabolism. ATGL is considered the central rate-limiting enzyme in the mobilization of fatty acids in mammals. Currently, severe fat accumulation has been commonly detected in farmed fish globally. However, the ATGL-mediated lipolysis and the potential synergy among ATGL, HSL, and autophagy, which is another way for lipid breakdown, have not been intensively understood in fish. In the present study, we added Atglistatin as an ATGL-specific inhibitor into the zebrafish diet and fed to the fish for 5 weeks. The results showed that the Atglistatin-treated fish exhibited severe fat deposition, reduced oxygen consumption, and fatty acid β-oxidation, accompanied with increased oxidative stress and inflammation. Furthermore, the Atglistatin-treated fish elevated total and phosphorylation protein expressions of HSL. However, the free fatty acids and lipase activities in organs were still systemically reduced in the Atglistatin-treated fish, and the autophagy marker LC3 was also decreased in the liver. On the other hand, glycogenolysis was stimulated but blood glucose was higher in the Atglistatin-treated fish. The transcriptomic analysis also provided the hint that the protein turnover efficiency in Atglistatin-treated fish was likely to be accelerated, but the protein content in whole fish was not affected. Taken together, ATGL plays crucial roles in energy homeostasis such that its inhibition causes loss of lipid-sourced energy production, which cannot be compensated by activation of HSL, autophagy, and utilization of other nutrients.

Keywords ATGL · Metabolism · Lipolysis · Autophagy · Energy homeostasis · Zebrafish

S.-L. Han · Y. Liu · S. M. Limbu · L.-Q. Chen · M.-L. Zhang · Z.-Y. Du (✉)
LANEH, School of Life Sciences, East China Normal University, Shanghai, China
e-mail: zydu@bio.ecnu.edu.cn

S. M. Limbu
Department of Aquatic Sciences and Fisheries Technology, University of Dar es Salaam, P.O. Box 35064, Dar es Salaam, Tanzania

S. M. Limbu
ECNU-UDSM Joint Research Center for Aquaculture and Fish Biology (JRCAFB), Dar es Salaam, Tanzania

Z.-Y. Du
ECNU-UDSM Joint Research Center for Aquaculture and Fish Biology (JRCAFB), Shanghai, China

Introduction

Patatin-like phospholipase domain containing 2 (PNPLA2) was discovered 17 years ago and designated as adipose triglyceride lipase (ATGL) (Zimmermann et al. 2004), which plays an important role in the initial step of lipolysis. It specifically hydrolyses triglycerides (TG) to diacylglycerol (DG) and releases a free fatty acid (FFA). The DG is further degraded by hormone-sensitive lipase (HSL) and monoglyceride lipase (MGL) into glycerol and FFAs (Fredrikson et al. 1986; Zechner

Published online: 27 November 2020

Author's personal copy

et al. 2012). Growing pieces of evidence demonstrate that dysregulated lipolysis is related to some metabolic disorders, such as fatty liver and type 2 diabetes (Cerk et al. 2018). In mammals, systemic ATGL-deficient mice were heavier than wild-type, showing enlarged fat depot both in brown (BAT) and white (WAT) adipose tissues and reduced FFAs in multiple tissues including muscle, testis, and liver (Haemmerle et al. 2006). Hepatocyte-specific ATGL deletion impairs FA oxidation and causes progressive hepatic steatosis (Wu et al. 2011), while overexpression of ATGL in liver ameliorates this condition (Reid et al. 2008). Moreover, lipid oxidation is also reduced in mice with adipocyte-specific ATGL deletion (Schoiswohl et al. 2015), in line with diet-induced obesity attenuated by overexpressed ATGL in adipose tissues (Ahmadian et al. 2009). Therefore, there is no doubt that ATGL is a key enzyme required in order to maintain energy homeostasis. Unlike ATGL, HSL exhibits much broader substrate because it is able to hydrolyze TG, MG, and CE as well (Kraemer and Shen 2006) and is hypothesized to play some compensatory effects for ATGL (Zhang et al. 2019), but this hypothesis has not been verified. Apart from the ATGL-HSL mediated lipolysis, lipophagy is another important pathway for lipid droplets (LDs) degradation and FFAs release (Singh and Cuervo 2012). Lipophagy works through the acid lipases in lysosome and has also been verified to play important roles in lipid-sourced energy production and energy homeostasis (Singh and Cuervo 2012). Besides, ATGL was reported to positively regulate autophagy/lipophagy and increase interactions of lysosomes and LC3 (microtubule associated light chain 3) with LDs in mammalian hepatocytes (Sathyanarayan et al. 2017). Therefore, lipophagy and ATGL are hypothesized to possess supplementary relations (Sathyanarayan et al. 2017). In fact, whether the functions of ATGL in energy metabolism can be compensated by activated HSL and autophagy remains unclear.

Excess fat accumulation and metabolic disorders have been a worldwide problem in farmed fish (Du et al. 2008; Yan et al. 2015) similar to mammals. Accordingly, the mechanisms for lipid breakdown and the related energy homeostasis have received extensive attention in fish. Indeed, ATGL, HSL, and MGL have been cloned in several fish species (Chen et al. 2014; Dai et al. 2018; Wang et al. 2013). The genes encoding for ATGL are conserved in a teleost (Sun et al. 2016) and contain the patatin domain with "GXSXG" motif as well, which are conservative structures of lipases (Smirnova et al. 2006). Supportably, the TG lipolysis in fish also occurs through the ATGL-HSL-MGL enzyme system, like mammals (Liu et al. 2015). However, the exact roles of ATGL in fish metabolism have not been investigated. Moreover, the synergy between ATGL and HSL has also not been elucidated in fish lipid metabolism. In addition, lipophagy has been recently verified to play essential roles in providing FFAs for energy production in fish (Wang et al. 2018; Wang et al. 2019). Nevertheless, the relationship between autophagy and ATGL-mediated lipolysis is also currently not known. On the other hand, the proportion of carbohydrates in energy metabolism of mammals is more than 50%, while their utilization is generally considered lower in fish (Stone 2003). In our previous studies, increased lipid-sourced energy production reduced glucose utilization and increased expression of mTOR (Li et al. 2017; Ning et al. 2016), which is a known maker of protein synthesis. These studies suggest that the modified lipid metabolism would affect glucose and protein metabolism to maintain energy homeostasis and the activities of some important pathways such as insulin signaling (e.g., insulin receptor, IR; phosphatidylinositol 3-kinase; PI3K) and mTOR pathway (e.g., mTOR and S6) may also vary accordingly. However, the exact roles of ATGL-mediated lipolysis in energy homeostasis have not been reported in fish. Specifically, there are several questions remained if ATGL is inhibited: (1) whether HSL would be stimulated to compensate for the dysfunction of ATGL; (2) whether autophagy would also be stimulated to compensate for the lowered LD degradation; and (3) whether the lowered lipid-soured energy supply would be compensated through elevating utilization of other nutrients, such as carbohydrate and/or protein? These are the questions which need to be answered in the present study.

Atglistatin (Mayer et al. 2013) is the first specific synthetic ATGL inhibitor, which has recapitulated many phenotypes of genetic mouse models (Schreiber et al. 2019), making pharmacological studies available in vitro and in vivo. Atglistatin treatment was also reported to attenuate hepatosteatosis in mice fed with high-fat diet (Schweiger et al. 2017), which may be due to its competitive or reversible inhibitory properties. Currently, zebrafish is a well-accepted animal model in medical and biological studies, and the metabolism data obtained from zebrafish has also been regarded as the important reference for clinical and animal nutrition (Faillaci et al. 2018; Williams and Watts 2019).

Author's personal copy

Therefore, in the present study, we used zebrafish as the animal model and Atglistatin as the specific ATGL inhibitor to investigate the effects of ATGL inhibition on nutrient metabolism and the potential compensatory responses of HSL and autophagy. Zebrafish were divided into two groups and fed with Atglistatin or not for 5 weeks. After the feeding trial, fish oxygen consumption rate, lipid deposition and composition, activities of FA β-oxidation and glycogen in liver and muscle, and fish protein and related signaling pathways were measured to verify the phenotypes on nutrient metabolism when ATGL was inhibited. The protein expressions of the total and phosphorylated HSL were detected to study the relationship between ATGL and HSL. Besides, Beclin1 and LC3 proteins were tested in liver through western blot or immunofluorescence to see if autophagy would be stimulated by ATGL suppression. Moreover, a whole fish transcriptomic analysis was performed to understand the regulatory pathways of Atglistatin in zebrafish. Finally, antioxidant capacities and inflammatory responses were detected to evaluate the potential lipotoxicity caused by ATGL inhibition. To the best of our knowledge, this is the first study to investigate the relationship among ATGL-mediated lipolysis, HSL, and autophagy in systemic energy homeostasis aspects.

Materials and methods

Fish, diets, and experimental design

Before the experiment, more than 600 zebrafish were purchased from the Chinese National Zebrafish Resource Center (Wuhan, China), acclimated for 2 weeks and fed with a commercial diet. In this study, only male zebrafish (initial mean weight: 0.17 ± 0.01 g) were selected for subsequent experiments in order to avoid the metabolic disturbance of estrogen during the sexual maturation of female fish. A basal diet was formulated to contain appropriate levels of nutrients for zebrafish growth and survival (see Supplementary Table 1). The Atglistatin (HY-15859, MedChemExpress (MCE)) was added to the small wheat flour-dough particles. In order to prepare the Atglistatin-containing wheat flour-dough particles, Atglistatin was first dissolved in dimethyl sulfoxide (DMSO), and the solution was mixed with the proper amount of wheat flour and water to make a wet dough to reach 0.32 mg Atglistatin/g wheat flour. The wet dough was rubbed into small particles with proper size for zebrafish, and then dried at 60 °C in an oven. The dosage of Atglistatin (final concentration 80 mg/kg diet) was set according to a previous reference (Mayer et al. 2013) and evaluated by our preliminary study, which showed no obvious toxic effects (see Supplementary Fig. 1). In the control diet, wheat flour-dough particles only contained the same volume of solvent (DMSO).

After acclimation, three hundred male zebrafish were randomly distributed into two treatments: control and Atglistatin (three replicates per treatment, 50 fish per replicate). Every morning, the fish in Atglistatin or control tanks were fed with the dough particles containing Atglistatin or not at 1% body weight daily, respectively. Afterward, the fish in the two treatments were fed with the basic diet at 3% body weight daily for 5 weeks. During the experiment, the water temperature was maintained at 28 ± 1 °C by an automatic heater with a 12-h light-dark cycle, and the dissolved oxygen, pH, and total ammonia nitrogen were maintained at ranges from 6.5 to 7.5 mg/L, 7.5 ± 0.5, and < 0.02 mg/L, respectively. The weight of all fish in each tank was recorded every week, and the feeding amount was adjusted correspondingly.

Sampling and the measurements of biochemical parameters

At the end of the trial, fish were fasted overnight and transferred to an oxygen-saturated water environment. The oxygen consumption rate (OCR) of live zebrafish was determined by Strathkelvin Instruments 782 Oxygen Meter System (North Lanarkshire, Scotland, UK). Afterward, all fish were euthanized and sampled to collect tissues for measurement of molecular, protein, and biochemical indexes in the liver, muscle, and viscera (without liver). The TG, glycogen, malondialdehyde (MDA), superoxide dismutase (SOD), reduced glutathione (GSH), lipase, and FFA were assessed by using specific commercial kits (Jiancheng Biotech Co., China). The blood glucose was assayed by using a blood glucose monitor (glucose dehydrogenase method, CONTOURTMPLUS Blood Glucose Monitoring Systems, Bayer). The total lipid of the whole fish body was extracted by using chloroform/methanol (2:1, v/v) and the lipid components, including neutral lipids and phospholipids, were subsequently separated by thin-layer chromatography (TLC). Whole fish protein and muscle protein were

Author's personal copy

measured by KjeltecTM 8200 (FOSS, Sweden). The total [^{14}-C] palmitate oxidation in liver and muscle homogenates was detected as described previously (Ning et al. 2016).

Nile Red, H&E, and PAS staining

Neutral lipid accumulation was visualized using Nile Red staining in live zebrafish as reported previously (Yang et al. 2017). Nile Red (N3013; Sigma) was dissolved in acetone at 2 mg/mL as the stock solution. Three fish from each treatment were dyed in 0.5 μg/mL Nile Red working solution at 28 °C for 3 h kept away from light. After that, the working solution was changed with clean water and washed after every 30 min for 3 h. Finally, fish were anesthetized and photographed. Images were obtained using an Olympus SZX16 FL stereomicroscope (Olympus, Tokyo, Japan) at an excitation wavelength of 488 nm. Pieces of livers and intestines were fixed in 4% paraformaldehyde and embedded in paraffin. Sections of 5 μm thickness were stained with the Harris hematoxylin–eosin (H&E) mixture by routine techniques. Additional unstained liver sections were used for periodic acid Schiff (PAS) staining and immunofluorescence.

Tissue immunofluorescence assays

The tissue immunofluorescence assays of liver were determined based on a previous article (Kajimura et al. 2016). The slides were immersed in xylene (5 min × 2) in order to remove paraffin, followed by graded ethanol (5 min × 2 in 100%, 5 min × 2 in 95%, then 5 min × 2 in 70% ethanol). Next, antigen retrieval was performed to enhance immunofluorescence signal intensity. After blocking for 30 min at room temperature, the primary antibody (anti-LC3A/B, #4108, CST) were added to the slice, they were placed in a wet box and incubated overnight at 4 °C. Then, the primary antibody was removed, and the sections were washed with PBS (pH 7.4, 5 min × 3), followed by the addition of secondary antibody and incubated at room temperature in the dark for an hour. They were then washed again three times; the nucleus was stained by 4′,6-diamidino-2-phenylindole (DAPI) and mounted with anti-fluorescence quencher and a cover-slip. Finally, images were collected under a Nikon inverted fluorescence microscope.

Quantitative real-time PCR

Total RNA of different tissues (liver, muscle, and viscera without liver) was isolated by using a TriPure Reagent (Aidlab, Beijing, China). The quality and quantity of total RNA were tested by a NANODROP 2000 Spectrophotometer (Thermo, USA) and only RNA with a 260/280 ratio > 1.9 was used for cDNA synthesis. The cDNAs were synthesized using a PrimerScript™ RT reagent Kit with a gDNA Eraser (RR047A, Takara, Shiga, Japan). Quantitative real-time PCR (qPCR) was performed as described previously (Han et al. 2020). The qPCR reaction consisted of 95 °C for 10 min, 40 cycles of 95 °C for 5 s, and 60 °C for 18 s. Elongation factor 1 alpha (*ef1α*) and *β-actin* were used as the reference genes, which were expressed stably among treatments. The primers of genes for qPCR were designed to overlap intron (Supplementary Table 2). The melting curves of amplified products were generated to ensure the specificity of assays at the end of each PCR. The qPCR efficiency was between 96 and 105% and the correlation coefficient was over 0.97 for each gene. The method of $2-\Delta\Delta Ct$ was used for estimating the relative cDNA abundance.

Western blotting

Liver homogenates were prepared by using the RIPA lysis buffer (Beyotime Biotechnology, China) for western blot (WB) analysis. Proteins were separated by using 8% or 12% sodium dodecyl sulfate-polyacrylamide gel electrophoresis (SDS-PAGE) and transferred electrophoretically to nitrocellulose membranes. Membranes were incubated for 1 h in a blocking solution containing 5% bovine serum albumin (BSA) in a mixture of tris-buffered saline (TBS) and polysorbate 20 (TBST). Membranes were washed briefly in a mixture of TBST and incubated overnight at 4 °C with the anti-HSL (1:800, #4107, CST), anti-p-HSL (Ser552) (1:800, D151508, BBI), anti-LC3A/B (1:800, #4108, CST), anti-Beclin1 (1:800, 11306-1-AP, Proteintech), anti-p-IRβ (Tyr1345) (1:800,#3026,CST), anti-IRβ (1:800, 20433-1-AP, Proteintech), anti-p-PI3K (Tyr458/199) (1:800, #4228, CST), anti-PI3K (1:800, CY6915, Abways), anti-p-mTOR (Ser2448) (1:800, #2971, CST), anti-mTOR (1:800, #2972, CST), anti-p-S6 (Ser235/236) (1;800, #4856, CST), anti-S6 (1:800, #2217, CST), and anti-GAPDH (1:3000, AB0036, Abways) antibodies. Afterwards, the blots were washed to remove excessive

Author's personal copy

primary antibody binding and finally were incubated for 1 h with horseradish peroxidase (HRP)–conjugated secondary antibody. The WB images were obtained by using the Odyssey CLx Imager (Licor, USA).

Transcriptomic analysis

The RNA for sequencing was collected from six RNA samples (whole fish) per treatment. Transcriptome sequencing was conducted by using Illumina HiSeq 2500 according to the manufacturer's instructions. After filtering out low-quality reads, the remaining clean reads were assembled and mapped to the zebrafish reference genome. Differential expression genes (DEGs) were calculated according to the fragments per kilobase of exon per million mapped reads (FRKM) method. The results of RNA-seq were validated by qPCR, in which several important genes referring to glucose, lipid, and protein metabolisms were selected, respectively (see Supplementary Fig. 2). Functional-enrichment analyses including Gene Ontology (GO) and Kyoto Encyclopedia of Genes and Genomes (KEGG) were performed to identify the DEGs that were significantly enriched in GO terms and metabolic pathways at Bonferroni-corrected P value ≤ 0.05 compared with the whole-transcriptome background.

Statistical analyses

Independent-samples t test was performed to evaluate the significant differences among measured variables between control and Atglistatin treatments ($P < 0.05$). All data were conducted using the SPSS Statistics 19.0 software (IBM, USA).

Results

ATGL inhibition caused severe lipid accumulation and reduced energy production

During the 5-week feeding trial, the Atglistatin-treated fish showed steady weight increase (Fig. 1a). Indeed, the Atglistatin-treated fish had significantly higher weight than control after the fourth week (Fig. 1a). Besides, Atglistatin-treated fish also increased condition factor (Fig. 1b), whole fish total lipid (Fig. 1c) and plasma TG (Fig. 1d) than control. Consistently, the Atglistatin-treated fish showed more abdominal fat deposition than control (Fig. 1e). Accordingly, the Atglistatin-treated fish had conspicuous white adipose tissue (AT) while the control zebrafish did not contain them (Fig. 1f–g). Moreover, the Atglistatin-treated fish liver showed much more vacuoles than the control (Fig. 1h). Furthermore, the Atglistatin-treated fish had higher TG contents in liver and muscle than control (Fig. 1i). The Atglistatin-treated fish also showed less OCR (Fig. 1j) and reduced β-oxidation activities in liver and muscle (Fig. 1k) than control. Altogether, ATGL inhibition caused severe lipid accumulation and reduced lipid catabolism.

ATGL inhibition changed lipid profile

The lipid profile of whole fish was changed significantly by Atglistatin treatment as shown in Fig. 2a–f. In the Atglistatin-treated fish, the TG and phospholipid (PL) increased significantly accompanied with a distinct decrease in FFA, DG, and MG, compared to the control. Among these variations, TG proportion contributed the largest change of lipid profile between Atglistatin and control (62% vs 53%) (Fig. 2f). Besides, the Atglistatin-treated fish had significantly lower concentration of FFA in the liver (Fig. 2g) and viscera without liver (Fig. 2h) than control. Therefore, ATGL inhibition changed lipid profile and reduced the availability of FFA for energy production.

ATGL inhibition caused slight increase in HSL functions but did not induce autophagy

The Atglistatin-treated fish decreased markedly the lipase activity in plasma (Fig. 3a) and viscera (Fig. 3b) than control. However, the Atglistatin-treated fish increased extremely the *atgl* gene expression in the liver (Fig. 3c) as a compensatory response, indicating that liver may be the main target organ for Atglistatin treatment in fish. Accordingly, the Atglistatin-treated fish reduced the hepatic expression of ATGL protein, while the expressions of P-HSL and T-HSL were elevated (Fig. 3d and e), suggesting that HSL can play a compensatory role in the degradation process of TG to DG when ATGL is inhibited (Fig. 3f). Besides, the liver of Atglistatin-treated fish showed fewer light spots after immunofluorescence images of LC3 than the control (Fig. 3g), and this was consistent with lower protein expressions of Beclin1 and LC3 in the liver in the same treatment than control (Fig. 3h and i). These results suggest that the ATGL inhibition increased HSL activity, but did not induce autophagy.

Author's personal copy

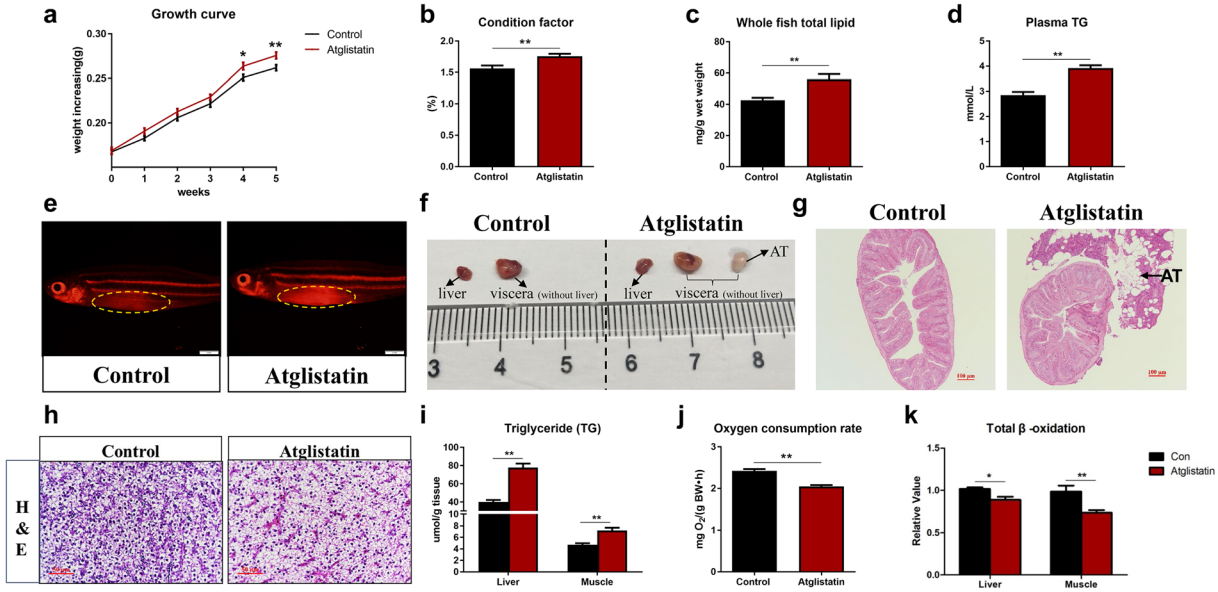


Fig. 1 The overall phenotypes of zebrafish after Atglistatin treatment. **a** growth curve; **b** condition factor: bodyweight × 100%/body length^3; **c** the total lipid content of whole fish; **d** plasma TG concentration; **e** pictures taken after Nile red staining, scale bars, 2 mm; **f** visceral dissection; **g** H&E staining of intestine and attached adipose tissue, scale bars, 100 μm; **h** H&E staining of liver, scale bars, 50 μm; **i** TG content in liver and muscle; **j** oxygen consumption rate (OCR) = [ΔO_2 concentration (mg /L) × water volume (L)]/[fish mass (g) × time (h)]; **k** total β-oxidation capability of [1-^{14}C] palmitate in the homogenates of liver and muscle. Values are means ± SEM ($n = 6$) except growth data ($n = 3$). Values with an asterisk and double asterisk indicate statistical differences at $P < 0.05$, and $P < 0.01$, respectively

ATGL inhibition reduced glycogen content without changing fish protein content

The Atglistatin-treated fish increased significantly the blood glucose concentration (Fig. 4a), while notably decreased the glycogen content in liver (Fig. 4c) and muscle (Fig. 4d) than control. Accordingly, the Atglistatin-treated fish showed lower pink positive reaction in the liver after glycogen-specific PAS staining than control (Fig. 4b). The Atglistatin-treated fish only downregulated the expression of T-PI3K protein involved in the insulin signaling pathway (Fig. 4e and f) than control. The Atglistatin-treated fish did not affect the whole fish protein content (Fig. 4g), although the hepatic expressions of P-mTOR and P-S6 increased markedly in this group (Fig. 4h–i).

ATGL inhibition caused systemic changes in nutrients metabolism

A transcriptomic assay was performed in the zebrafish treated with Atglistatin or not. The well-matched qPCR analyses of 16 gene expressions indicated the reliability of the RNA-Seq data (see Supplementary Fig. 2). A total of 1349 DEGs were differentially expressed compared with the control. These DEGs were further analyzed by KEGG enrichment to distinguish biological processes. The most predominantly affected process was "metabolism" (92%) in which amino acid, lipid, and carbohydrate metabolisms occupied comparatively similar large portions (Fig. 5a). The number of the significantly changed genes in three major metabolisms was amino acid, followed by lipid, and carbohydrate (Fig. 5b). In general, more genes were upregulated than those downregulated.

We then filtered the dramatically changed genes of three metabolisms ($P < 0.05$ & $|\log2\text{FoldChange}| \geq 2$) to evaluate the possible variation trends (Fig. 5c–e). Most of genes were related to amino acid catabolism (Fig. 5c). The Atglistatin-treated fish upregulated serine or cysteine proteinase inhibitor (*serpina*) gene compare to control. Several important genes involved in amino acid turnover, such as *gpt2l*, *glud1b*, and *tat*, were induced (Fig. 6). More drastic transcript changes were obtained in lipid metabolism (Fig. 5d). Many genes related to lipid synthesis, such as *acaca*, *lcat*, *fads2*, *elovl*, and *mogat3a*, were upregulated, and apolipoprotein genes, including *apob* and *apoea*, were also highly increased in

Author's personal copy

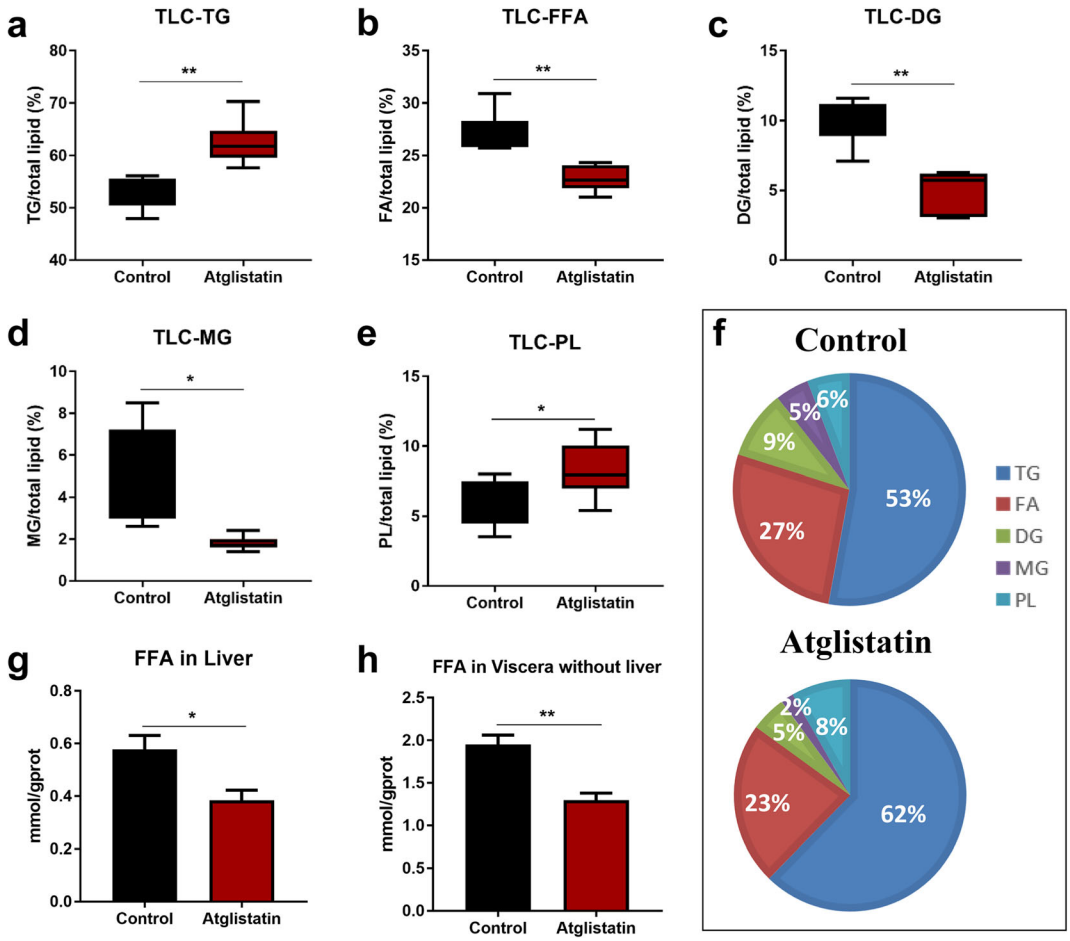


Fig. 2 Effects of Atglistatin treatment on lipid profile of whole fish and tissues. **a** The percentage of triglyceride (TG) to total lipid ($n = 8$); **b** the percentage of free fatty acid (FFA) to total lipid ($n = 8$); **c** the percentage of diacylglycerol (DG) to total lipid ($n = 8$); **d** the percentage of monoglyceride (MG) to total lipid ($n = 8$); **e** the percentage of phospholipid (PL) to total lipid ($n = 8$); **f** the average proportion of lipid class composition; **g** FFA content in liver ($n = 6$); **h** FFA in viscera without liver ($n = 6$). Values with an asterisk and double asterisk indicate statistical differences at $P < 0.05$ and $P < 0.01$, respectively

Atglistatin-treated fish than control. However, *pnpla2* (*atgl*), *lipe* (*hsl*), and mitochondrial FA β-oxidation (*cpt*, *acadl*, *hadha*) genes had no significant differences at the transcriptome level (Fig. 6) between the two treatments. Instead, the Atglistatin-treated fish increased other lipase genes such as *cel*, *lipca*, *lpl*, and peroxisomal β-oxidation genes (*acaa*, *acox1*, *ehhadh*) as compensatory responses. In regard to glucose metabolism, the Atglistatin-treated fish upregulated the genes related to gluconeogenesis (*pck1*, *fbp1b*, *g6pca.2*) compared to the control (Fig. 5e). Besides, the Atglistatin-treated fish downregulated important glycolysis-related genes, such as hexokinase (*hk1*) and phosphofructokinase (*pfkmb*) than control (Fig. 5e). In addition, the Atglistatin-treated fish increased significantly the glycogen phosphorylase, liver (*pygl*), glycogen synthase 2 (*gys2*) genes, and several genes involved in the TCA cycle (*aco1*, *idh1*) (Fig. 6). These results suggested that the ATGL-inhibited zebrafish increased turnover of glycogen and protein, but did not increase glucose breakdown.

ATGL inhibition triggered oxidative stress and lipotoxicity

Several indexes related to oxidative stress were determined in the liver. The Atglistatin-treated fish increased slightly MDA content (Fig. 7a), but had significantly lower GSH (Fig. 7b) and SOD (Fig. 7c) than control. Furthermore, two inflammatory factors, *tnf-α* and *il-1β*, were assayed in liver and the former gene (*tnf-α*) had

Author's personal copy

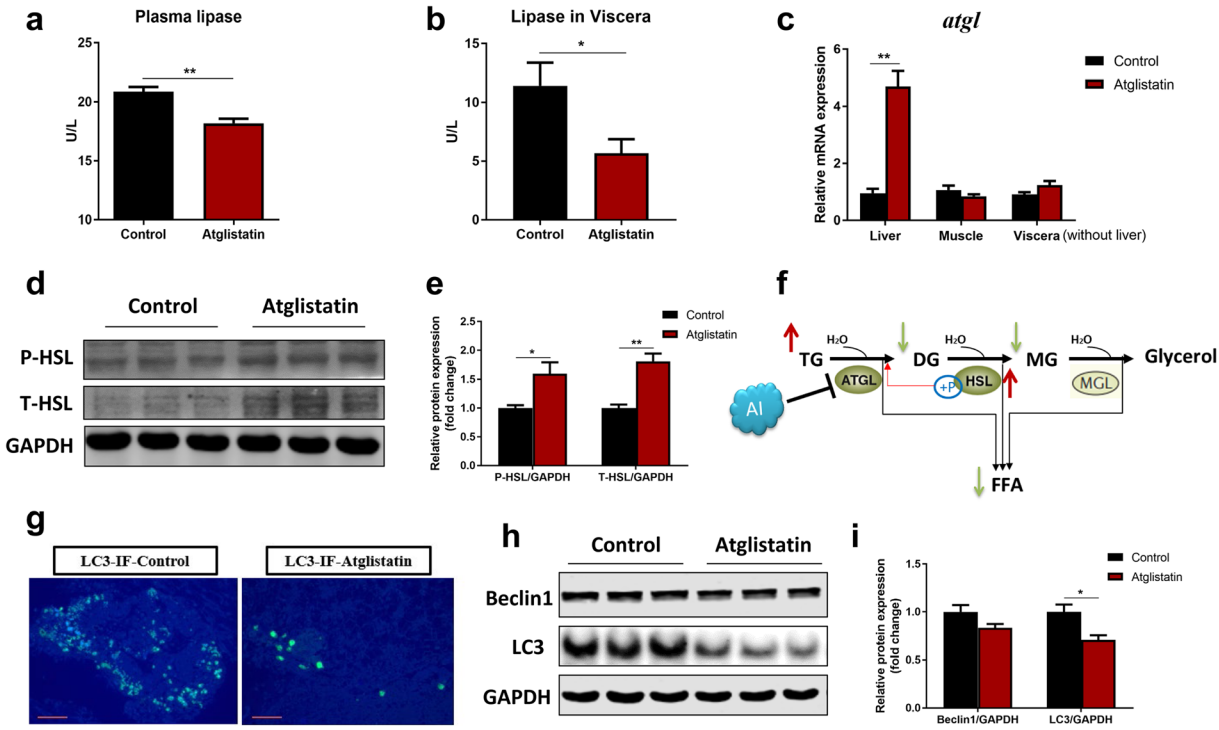


Fig. 3 Effects of Atglistatin treatment on lipolysis and autophagy in zebrafish. **a** lipase activity in plasma; **b** lipase activity in viscera; **c** the gene expression of atgl in liver, muscle, and viscera without liver, respectively; **d**, **e** the protein expressions of p-HSL and T-HSL in liver; **f** the potential relationship between ATGL and HSL in zebrafish liver; **g** immunofluorescence (IF) of LC3 in liver, the image magnification is × 400, scale bars, 50 μm; **h**, **i** the protein expressions of Beclin1 and LC3 in liver. Values are means ± SEM ($n = 6$). Values with an asterisk and double asterisk indicate statistical differences at $P < 0.05$ and $P < 0.01$, respectively

much higher expression in the Atglistatin group (Fig. 7d). Similar changes in the Atglistatin-treated fish were also found in the viscera (without liver), for higher MDA (Fig. 7e), decreased SOD (Fig. 7f), GSH (Fig. 7g) activities, and higher *tnf-α* expression (Fig. 7h). All these data deliver a message that the inhibited ATGL by Atglistatin triggered oxidative stress and inflammation.

Discussion

The role of ATGL in lipid metabolism

Abnormal lipolysis (Wu et al. 2011; Xia et al. 2017) causes an imbalance between lipid storage and TG mobilization and, thus, induces obesity. Excessive fat accumulation is closely related to metabolic syndromes like fatty liver, hyperlipidemia, and cardiovascular disease (Van Herpen and Schrauwen-Hinderling 2008). In the present study, the inhibition of ATGL caused severe lipid deposition in different tissues of fish as shown in Fig. 1. Similar lipid storage phenotype was also observed in CGI-58$^{-/-}$ (an ATGL co-activator) mice, whereby the intestinal CGI-58 deficiency mice exhibited impaired fatty acid absorption and reduced postprandial TG secretion (Xie et al. 2014). In the present work, the intestinal adipose tissue only appeared in the Atglistatin-treated fish, implying reduced lipolysis capacity in this tissue. Simultaneously, the FFA content in tissues was significantly reduced, showing the inhibited lipolysis systemically reduced the availability of FFA as the basic substrate for energy production. Accordingly, our data showed that the oxygen consumption rate and FA β-oxidation in liver and muscle were both reduced significantly by the Atglistatin treatment. This FFA deficiency caused lowered lipid catabolism and energy production has also been demonstrated in our previous zebrafish study, in which the lipophagic process was inhibited (Wang et al. 2018).

Consistently, ATGL deficiency in the mice heart not only caused cardiac lipid accumulation but also disrupted mitochondrial substrate oxidation and respiration, while PPAR-α agonists like WY14643 and fenofibrate reversed the mitochondrial defects

Author's personal copy

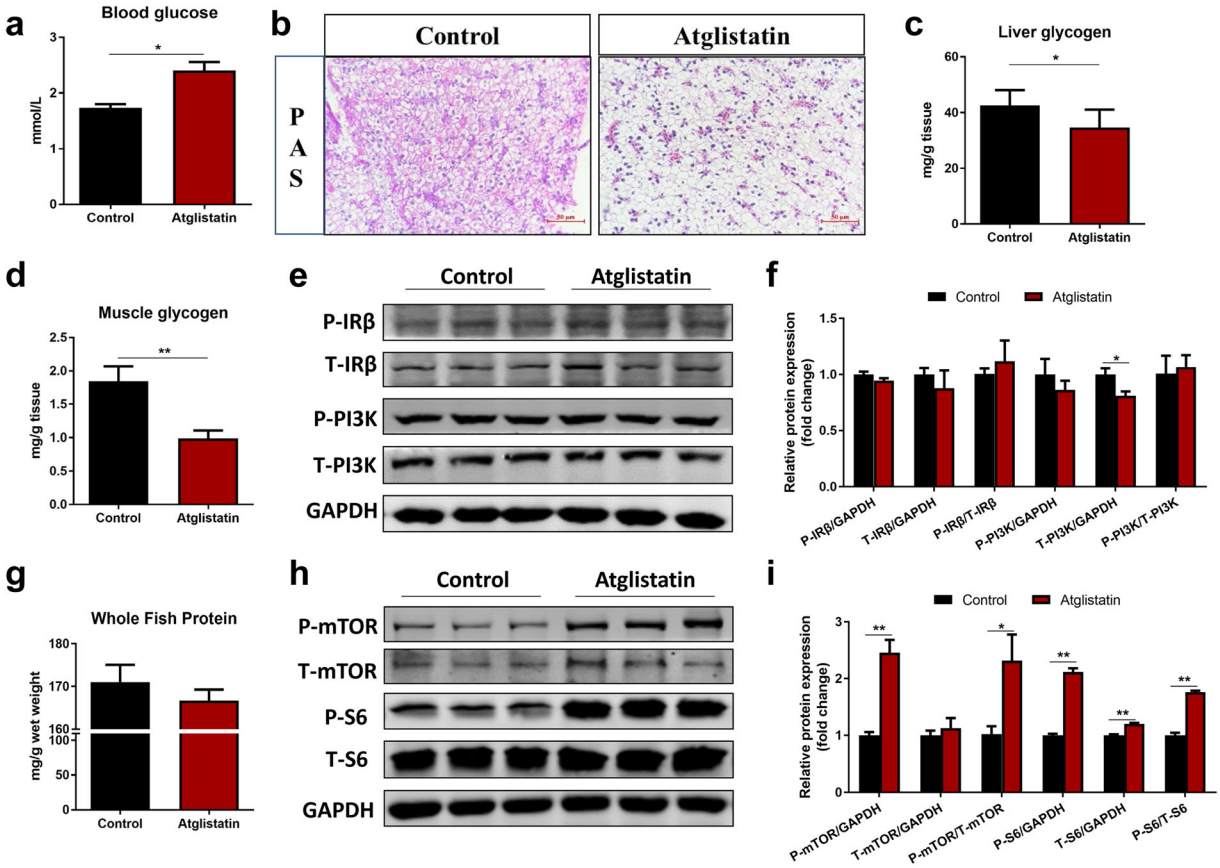


Fig. 4 The effect of Atglistatin supplementation on glucose and protein metabolism. **a** Blood glucose concentration; **b** PAS staining of liver, scale bars, 50 μm; **c** glycogen content in liver; **d** glycogen in muscle; **e**, **f** the protein expressions of P-IRβ, T-IRβ, P-PI3K, and T-PI3K in liver; **g** the protein content of whole zebrafish; **h**, **i** the protein expression of P-mTOR, T-mTOR, P-S6, and T-S6. Values are means ± SEM ($n = 6$). Values with an asterisk and double asterisk indicate statistical differences at $P < 0.05$, $P < 0.01$, respectively

(Haemmerle et al. 2011). In the ATGL$^{-/-}$ mice, decreased expressions of PPARα target genes were also found in several tissues such as liver (Ong et al. 2011), intestine (Obrowsky et al. 2013), and heart (Haemmerle et al. 2011). In the present study, the PPARα and some genes related to mitochondrial β-oxidation at the transcriptome level did not change (Fig. 6). However, several peroxisomal β-oxidation genes (*acaa*, *acox1*, *ehhadh*) were all upregulated. These results suggest dysfunction of mitochondria because peroxisomal β-oxidation is usually upregulated when mitochondrial activities are impaired (Du et al. 2013). In addition, hepatocyte-specific CGI-58 knockout mice not only caused hepatic steatosis but also developed steatohepatitis and fibrosis, evidenced by the extremely high expression of inflammation-related genes in the liver (Guo et al. 2013). Similarly, significantly increased oxidative stress and inflammatory response (high mRNA expression of *tnf-α*) were also obtained in the Atglistatin-treated zebrafish. In fact, the high oxidative stress and inflammation have been tightly correlated with severe fat accumulation in organs, named as lipotoxicity (Reue 2011; Van Herpen and Schrauwen-Hinderling 2008). All these verify that the ATGL inhibition reduced lipid-sourced energy production caused severe fat accumulation and triggered lipotoxicity.

The relationship between ATGL and HSL in lipolysis

Previously, HSL was thought to be the main enzyme in TG hydrolysis (Raben and Baldassare 2005). However, HSL-deficient mice were lean and DG was abundant instead of TG accumulation (Haemmerle et al. 2002), indicating that other enzymes may be responsible for TG mobilization. Later, ATGL was discovered in mammals and was reported to express predominantly in

Author's personal copy

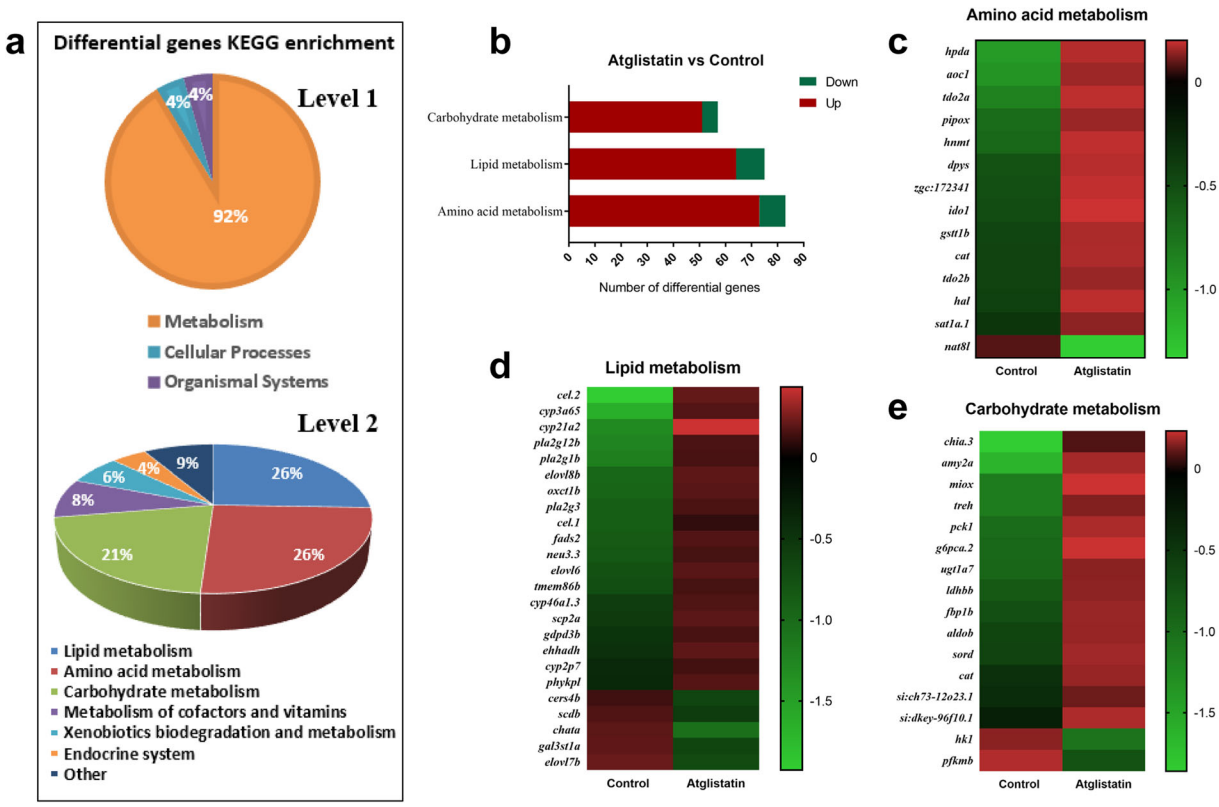


Fig. 5 Transcriptomic analysis of the nutrient metabolism in the ATGL-inhibited fish. **a** DEG category distribution (Atglistatin vs control); **b** the number of up- or downregulated DEGs in three major nutrient metabolisms; **c**, **d**, **e** the dramatically changed genes of amino acid metabolism, lipid metabolism, and carbohydrate metabolism ($P < 0.05$ & $|\log2\text{FoldChange}| \geq 2$)

white and brown adipose tissues, and to a lesser extent in non-adipose tissues, such as liver, muscle, heart (Zimmermann et al. 2004), and small intestine (Obrowsky et al. 2013). Unlike mammals, the gene expression of *atgl* in the present study varied dramatically only in liver after Atglistatin treatment in line with the results in other fish species (Dai et al. 2018; Sun et al. 2016), in which ATGL was highly expressed in liver and muscle rather than adipose tissue. Currently, ATGL and HSL are known as two committed enzymes in lipolytic cascade but with different substrate preferences (Schweiger et al. 2006). The ATGL specifically hydrates TG, especially cleaving ester bonds in the sn-1 or sn-2 position, while HSL prefers sn-1 or sn-3 position of DG, and is able to hydrolyze TG, MG, and cholesteryl esters as well (Lafontan and Langin 2009; Rodriguez et al. 2010). Therefore, ATGL and HSL seem to be complementary in theory. In fact, a previous research showed accelerated protein expression of P-HSL during fasting in the WAT from specific ATGL-adipose-deficient (ATGLAKO) mice, presumably due to mobilization of TG through the mediation of HSL (Wu et al. 2012). However, another study demonstrated that FFA and glycerol release were drastically reduced in WAT from ATGL$^{-/-}$ mice compared with the wild-type in the presence of isoproterenol (Haemmerle et al. 2006), suggesting that the alternative lipases such as HSL may not efficiently compensate for the loss of ATGL. Similarly, in the present study, in the Atglistatin-treated zebrafish, lipase activities measured in plasma and viscera were both significantly decreased, and whole fish TG increased by 9% (from 53% in control to 62% in Atglistatin treatment) while DG decreased by 4% (from 9% in control to 5% in Atglistatin treatment). Although the P-HSL and T-HSL were elevated in liver, and the transcriptome data also showed that other lipases, such as *cel*, *lipca*, and *lpl* were upregulated, the overall reduced FFA concentrations in organs verified that the partial increased activity of HSL or other lipases could not reverse the lipolysis reduction caused by ATGL inhibition.

Author's personal copy

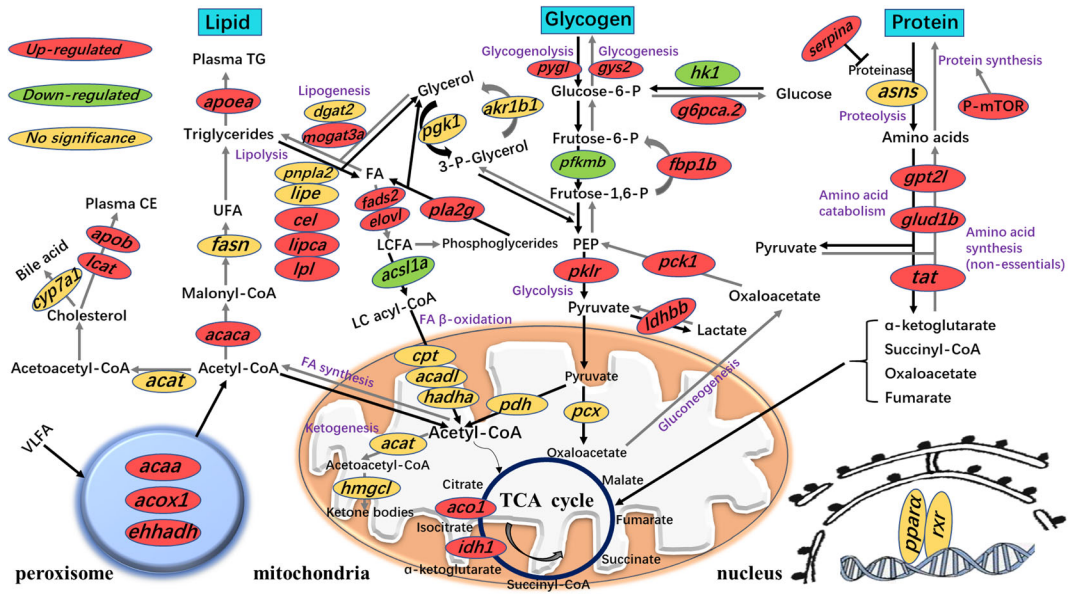


Fig. 6 Systemic regulation of Atglistatin in metabolic pathways. *cyp7a1*, cytochrome P450, family 7, subfamily A, polypeptide1; *lcat*, lecithin-cholesterol acyltransferase; *apob*, apolipoprotein Ba/ apolipoprotein Bb; *acat*, acetyl-CoA acetyltransferase; *acaca*, acetyl-CoA carboxylase alpha; *acaa*, acetyl-CoA acyltransferase 1/2; *acox1*, acyl-CoA oxidase 1, palmitoyl; *ehhadh*, enoyl-CoA, hydratase/3-hydroxyacyl CoA dehydrogenase; *fasn*, fatty acid synthase; *apoea*, apolipoprotein Ea; *pnpla2*, patatin-like phospholipase domain containing 2 (atgl); *lipe*, lipase, hormone-sensitive a/b (hsl); *cel*, carboxyl ester lipase, tandem duplicate 1/2; *lipca*, lipase, hepatic a; *lpl*, lipoprotein lipase; *dgat2*, diacylglycerol O-acyltransferase 2; *mogat3a*, monoacylglycerol O-acyltransferase 3a; *fads2*, fatty acid desaturase 2; *elovl*, ELOVL fatty acid elongase 2/5/6/8b; *acsl1a*, acyl-CoA synthetase long chain family member 1a; *pla2g*, phospholipase A2, group IB/III/ XIIB; *pgk1*, phosphoglycerate kinase 1; *akr1b1*, aldo-keto reductase family 1, member B1; *cpt*, carnitine palmitoyl transferase; *acadl*, acyl-CoA dehydrogenase long chain; *hadha*, hydroxyacyl CoA dehydrogenase trifunctional multienzyme complex subunit alpha; *hmgcl*, 3-hydroxy-3-methylglutaryl-CoA lyase; *pdh*, pyruvate dehydrogenase; *aco1*, aconitase 1, soluble; *idh1*, isocitrate dehydrogenase 1 (NADP+), soluble; *pcx*, pyruvate carboxylase a/b; *pklr*, pyruvate kinase L/R; *ldhbb*, lactate dehydrogenase Bb; *pck1*, phosphoenol-pyruvate carboxykinase 1 (soluble); *pfkmb*, phosphofructokinase, muscle b; *fbp1b*, fructose-1,6-bisphosphatase 1b; *g6pca.2*, glucose-6-phosphatase a, catalytic subunit, tandem duplicate 2; *hk1*, hexokinase 1; *gys2*, glycogen synthase 2; *pygl*, phosphorylase, glycogen, liver; *serpina*, serpin peptidase inhibitor, clade A (alpha-1antiproteinase, antitrypsin), member 1/7; *asns*, asparagine synthetase; *gpt2l,* glutamic pyruvate transaminase (alanine amino transferase) 2, like; *glud1b*, glutamate dehydrogenase 1b; *tat*, tyrosine aminotransferase; *ppara*, peroxisome proliferator-activated receptor alpha a/b; *rxr*, retinoid x receptor alpha a/b, beta a/b

Complex interaction between ATGL and autophagy

So far, lipolysis and lipophagy are two primary mechanisms for mobilizing FAs from TGs (Rambold et al. 2015; Singh and Cuervo 2012). Many studies in mammals have stated that lipophagy is an important pathway for TG breakdown in lipid metabolism (Schulze et al. 2017; Zhang et al. 2018), and the same is true in fish (Wang et al. 2018; Zhao et al. 2019). A previous research found that cold-induced autophagy facilitated lipolysis via LC3 coupled with ATGL in brown adipocytes (Martinez-Lopez et al. 2016), highlighting the possible crosstalk between autophagy and lipolysis. However, by using AOHO mice (both ATGL and HSL deficiency), another research demonstrated that autophagy and lipolysis were not necessarily alternative (Goeritzer et al. 2015). In the present work, autophagy marker protein LC3 was obviously decreased in the liver of the Atglistatin-treated zebrafish, indicating that autophagy was not activated by the ATGL inhibition. Several reasons may account for this result. First, ATGL may directly promote autophagy/lipophagy through signaling of PPAR-α and SIRT1(Lee et al. 2008; Lee et al. 2014; Sathyanarayan et al. 2017), so the inhibition of ATGL itself is possible to interfere with autophagic function. Second, other signaling factors, such as mTOR and AMPK, and hormones can also regulate autophagy (Zechner et al. 2017) similar to the regulation of lipolysis. In the present study, increased protein expression of p-mTOR, which is the negative upstream regulator of autophagy, might contribute to the depressed autophagy. Furthermore, overloaded lipid deposition also can

Author's personal copy

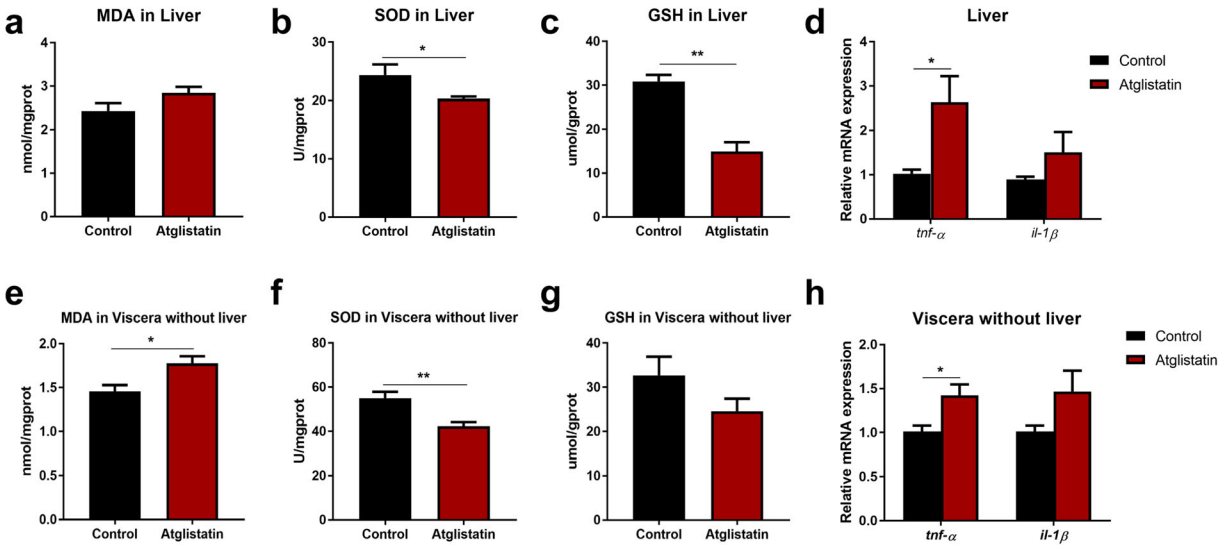


Fig. 7 The effects of Atglistatin on antioxidant capacity and inflammation. **a** Malondialdehyde (MDA) in liver; **b** superoxide dismutase (SOD) in liver; **c** glutathione (GSH) in liver; **d** *tnf-a* and *il-1β* mRNA levels in liver; **e** MDA in viscera without liver; **f** SOD in viscera without liver; **g** GSH in viscera without liver; **h** *tnf-a* and *il-1β* mRNA levels in viscera without liver. Values are means ± SEM ($n = 6$). Values with an asterisk and double asterisk indicate statistical differences at $P < 0.05$, $P < 0.01$, respectively

decrease the expression of LC3, as previously reported in mice (Yang et al. 2010) and fish liver (Han et al. 2020). Taken together, although the relationship between ATGL and autophagy/lipophagy is complicated, at least in the present study, the inhibited ATGL did not induce the compensatory increase of autophagy. Further studies are still needed in order to fully understand the relationship between ATGL and autophagy/lipophagy in fish.

Regulation of ATGL on glucose and protein metabolism in fish

Glucose and lipid metabolism are interlinked because insulin resistance is common in patients with severe fat accumulation (Parhofer 2015; Perry et al. 2014). Therefore, abnormal lipolysis may influence glucose homeostasis. Our initial hypothesis was that if lipolysis is blocked in fish, the energy sourced from other nutrients, for example glycogen degradation, would compensate for the lack of FFA breakdown. In our experimental data, glycogen in liver and muscle decreased significantly in the Atglistatin-treated fish, suggesting that the Atglistatin-treated fish used glycogen when FFA was inadequate for energy supply. However, blood glucose was elevated in the Atglistatin-treated zebrafish. This suggests that although the Atglistatin-treated zebrafish elevated glycogen degradation to release more glucose, the increased glucose could not be efficiently used for final energy production. Accordingly, the activity of the insulin signaling pathway detected in liver was not significantly affected by the Atglistatin treatment except for the decreased T-PI3K (Fig. 4e and f). In addition, gluconeogenesis-related genes in Atglistatin-treated fish such as *pck1*, *fbp1b*, and *g6pca2* were highly upregulated while *hk1* and *pfkmb* as key enzymes involved in glycolysis were significantly downregulated at the transcriptome level (Fig. 6). Therefore, the inhibition of ATGL in fish seems merely to promote glycogenolysis without facilitating glucose utilization for energy production.

However, different from our fish, the mice with systemic ATGL deletion showed improved glucose tolerance and enhanced insulin sensitivity despite severe TG accumulation (Haemmerle et al. 2006; Kienesberger et al. 2009). Nevertheless, the activity of the insulin signaling pathway in the ATGL-deficient mice was increased in skeletal muscle and WAT, but decreased in BAT and liver (Kienesberger et al. 2009), showing that the effects of ATGL deficiency on insulin signaling are tissue-dependent. In addition, the adenovirus-mediated liver ATGL overexpression in obese mice decreased hepatic steatosis and mildly improved liver insulin sensitivity (Turpin et al. 2011). Moreover, FFAs are demonstrated to be critical for glucose-stimulated insulin secretion (GSIS); thus, the pharmacological

Author's personal copy

ATGL inhibition (Schweiger et al. 2017) and systemic ATGL knockout in mice showed extremely low plasma insulin concentrations (Peyot et al. 2009). Furthermore, adipose-specific ATGL-deficient mice had reduced plasma FAs and insulin upon fasting (Wu et al. 2012), and β-cell-specific ATGL knockout mice exhibited impaired GSIS and decreased plasma insulin as well (Attané et al. 2016). Therefore, the decreased insulin signaling pathway activity in the present study is probably related to the reduction of insulin secretion because of the lowered FFA release from TG in the ATGL-inhibited fish. As for the protein metabolism, the whole fish total protein was comparable between the two treatments in the present study. Although the protein expression of P-mTOR, which is closely related with protein synthesis, was increased in the Atglistatin-treated fish, the mRNA of a series of genes involved in amino acid turnover, such as *gpt2l*, *glud1b*, *tat* (Fig. 6), and amino acid catabolism (*hnmt*, *ido1*, *pipox*, *tdo2a/b*, *hal*, *hpda*, etc.) were extremely highly expressed (Fig. 5c). Therefore, these data indicate that the ATGL inhibition might accelerate protein turnover efficiency, although the protein content was relatively stable. However, considering the oxygen consumption was still lower in the Atglistatin-treated fish, the accelerated protein turnover was not likely to supply sufficient energy to offset the loss of lipid-sourced energy caused by ATGL inhibition.

Conclusion

The present results demonstrated that the Atglistatin-induced inhibition of ATGL in zebrafish caused severe fat accumulation, reduced oxygen consumption rate and FA β-oxidation, accompanied by increased oxidative stress and inflammation. The partial increased HSL failed to reverse the effects caused by ATGL inhibition, and the compensatory autophagy increase was not obtained. The ATGL inhibition also accelerated glycogenolysis and protein turnover, without affecting the fish protein content, however reducing the expressions of glycolysis-related genes. Therefore, ATGL is a crucial enzyme in metabolic homeostasis, and its inhibition causes loss of lipid-sourced energy production, which cannot be compensated by activation of HSL, autophagy, and utilization of other nutrients.

Supplementary Information The online version contains supplementary material available at https://doi.org/10.1007/s10695-020-00904-7.

Author contributions ZY. D. and SL. H. conceived the study and designed the experiments. SL. H. carried out the experiments, analyzed the data, and wrote the manuscript. Y. L., LQ. C., and ML. Z. contributed reagents/materials/analysis tools. SL. H., S. M. L., and ZY. D. wrote and revised the manuscript. All authors read and approved the final manuscript.

Funding This work was financed by the National Natural Science Fund of China (31830102) and the Program of Shanghai Academic Research Leader (19XD1421200).Data availabilityThe data and materials that support the findings of this study are available from the corresponding author upon reasonable request.

Compliance with ethical stands All experiments were conducted strictly under the Guidance of the Care and Use of Laboratory Animals in China. This study was approved by the Committee on the Ethics of Animal Experiments of East China Normal University (Approval ID: F20140101).

Conflict of interest The authors declare that they have no conflicts of interest.

References

Ahmadian M, Duncan RE, Varady KA, Frasson D, Hellerstein MK, Birkenfeld AL, Samuel VT, Shulman GI, Wang Y, Kang C (2009) Adipose overexpression of desnutrin promotes fatty acid use and attenuates diet-induced obesity. Diabetes 58:855–866. https://doi.org/10.2337/db08-1644

Attané C, Peyot ML, Lussier R, Poursharifi P, Zhao S, Zhang D, Morin J, Pineda M, Wang S, Dumortier O (2016) A beta cell ATGL-lipolysis/adipose tissue axis controls energy homeostasis and body weight via insulin secretion in mice. Diabetologia 59:2654–2663. https://doi.org/10.1007/s00125-016-4105-2

Cerk IK, Wechselberger L, Oberer M (2018) Adipose triglyceride lipase regulation: an overview. Curr Protein Pept Sci 19:221–233. https://doi.org/10.2174/1389203718666170918160110

Chen QL, Luo Z, Song YF, Wu K, Huang C, Pan YX, Zhu QL (2014) Hormone-sensitive lipase in yellow catfish *Pelteobagrus fulvidraco*: molecular characterization, mRNA tissue expression and transcriptional regulation by leptin in vivo and in vitro. Gen Comp Endocrinol 206:130–138. https://doi.org/10.1016/j.ygcen.2014.06.031

Dai YJ, Liu WB, Li XF, Zhou M, Xu C, Qian Y, Jiang GZ (2018) Molecular cloning of adipose triglyceride lipase (ATGL) gene from blunt snout bream and its expression after LPS-induced TNF-α factor. Fish Physiol Biochem 44:1143–1157. https://doi.org/10.1007/s10695-018-0502-4

Author's personal copy

Du ZY, Clouet P, Huang L, Degrace P, Zheng W, He J, Tian L, Liu Y (2008) Utilization of different dietary lipid sources at high level in herbivorous grass carp (*Ctenopharyngodon idella*): mechanism related to hepatic fatty acid oxidation. Aquac Nutr 14:77–92. https://doi.org/10.1111/j.1365-2095.2007.00507.x

Du ZY, Ma T, Liaset B, Keenan AH, Araujo P, Lock EJ, Demizieux L, Degrace P, Frøyland L, Kristiansen K, Madsen L (2013) Dietary eicosapentaenoic acid supplementation accentuates hepatic triglyceride accumulation in mice with impaired fatty acid oxidation capacity. Biochim Biophys Acta 1831:291–299. https://doi.org/10.1016/j.bbalip.2012.10.002

Faillaci F, Milosa F, Critelli RM, Turola E, Schepis F, Villa E (2018) Obese zebrafish: a small fish for a major human health condition. Anim Model Exp Med 1:255–265. https://doi.org/10.1002/ame2.12042

Fredrikson G, Tornqvist H, Belfrage P (1986) Hormone-sensitive lipase and monoacylglycerol lipase are both required for complete degradation of adipocyte triacylglycerol. Biochim Biophys Acta 876:288–293. https://doi.org/10.1016/0005-2760(86)90286-9

Goeritzer M, Vujic N, Schlager S, Chandak PG, Korbelius M, Gottschalk B, Leopold C, Obrowsky S, Rainer S, Doddapattar P (2015) Active autophagy but not lipophagy in macrophages with defective lipolysis. Biochim Biophys Acta 1851:1304–1316. https://doi.org/10.1016/j.bbalip.2015.06.005

Guo F, Ma Y, Kadegowda AK, Betters JL, Xie P, Liu G, Liu X, Miao H, Ou J, Su X (2013) Deficiency of liver comparative gene identification-58 causes steatohepatitis and fibrosis in mice. J Lipid Res 54:2109–2120. https://doi.org/10.1194/jlr.M035519

Haemmerle G, Zimmermann R, Hayn M, Theussl C, Waeg G, Wagner E, Sattler W, Magin TM, Wagner EF, Zechner R (2002) Hormone-sensitive lipase deficiency in mice causes diglyceride accumulation in adipose tissue, muscle, and testis. J Biol Chem 277:4806–4815. https://doi.org/10.1074/jbc.M110355200

Haemmerle G, Lass A, Zimmermann R, Gorkiewicz G, Meyer C, Rozman J, Heldmaier G, Maier R, Theussl C, Eder S (2006) Defective lipolysis and altered energy metabolism in mice lacking adipose triglyceride lipase. Science 312:734–737. https://doi.org/10.1126/science.1123965

Haemmerle G, Moustafa T, Woelkart G, Büttner S, Schmidt A, Van De Weijer T, Hesselink M, Jaeger D, Kienesberger PC, Zierler K (2011) ATGL-mediated fat catabolism regulates cardiac mitochondrial function via PPAR-α and PGC-1. Nat Med 17:1076–1085. https://doi.org/10.1038/nm.2439

Han SL, Wang J, Li LY, Lu DL, Chen LQ, Zhang ML, Du ZY (2020) The regulation of rapamycin on nutrient metabolism in Nile tilapia fed with high-energy diet. Aquaculture 520:734975. https://doi.org/10.1016/j.aquaculture.2020.734975

Kajimura J, Ito R, Manley NR, Hale LP (2016) Optimization of single-and dual-color immunofluorescence protocols for formalin-fixed, paraffin-embedded archival tissues. J Histochem Cytochem 64:112–124. https://doi.org/10.1369/0022155415610792

Kienesberger PC, Lee D, Pulinilkunnil T, Brenner DS, Cai L, Magnes C, Koefeler HC, Streith IE, Rechberger GN, Haemmerle G (2009) Adipose triglyceride lipase deficiency causes tissue-specific changes in insulin signaling. J Biol Chem 284:30218–30229. https://doi.org/10.1074/jbc.M109.047787

Kraemer FB, Shen WJ (2006) Hormone-sensitive lipase knockouts. Nutr Metab 3:12. https://doi.org/10.1186/1743-7075-3-12

Lafontan M, Langin D (2009) Lipolysis and lipid mobilization in human adipose tissue. Prog Lipid Res 48:275–297. https://doi.org/10.1016/j.plipres.2009.05.001

Lee IH, Cao L, Mostoslavsky R, Lombard DB, Liu J, Bruns NE, Tsokos M, Alt FW, Finkel T (2008) A role for the NAD-dependent deacetylase Sirt1 in the regulation of autophagy. Proc Natl Acad Sci U S A 105:3374–3379. https://doi.org/10.1073/pnas.0712145105

Lee JM, Wagner M, Xiao R, Kim KH, Feng D, Lazar MA, Moore DD (2014) Nutrient-sensing nuclear receptors coordinate autophagy. Nature 516:112–115. https://doi.org/10.1038/nature13961

Li JM, Li LY, Qin X, Ning LJ, Lu DL, Li DL, Zhang ML, Wang X, Du ZY (2017) Systemic regulation of L-carnitine in nutritional metabolism in zebrafish, *Danio rerio*. Sci Rep 7:40815. https://doi.org/10.1038/srep40815

Liu D, Mai K, Ai Q (2015) Tumor necrosis factor alpha is a potent regulator in fish adipose tissue. Aquaculture 436:65–71. https://doi.org/10.1016/j.aquaculture.2014.10.030

Martinez-Lopez N, Garcia-Macia M, Sahu S, Athonvarangkul D, Liebling E, Merlo P, Cecconi F, Schwartz GJ, Singh R (2016) Autophagy in the CNS and periphery coordinate lipophagy and lipolysis in the brown adipose tissue and liver. Cell Metab 23:113–127. https://doi.org/10.1016/j.cmet.2015.10.008

Mayer N, Schweiger M, Romauch M, Grabner GF, Eichmann TO, Fuchs E, Ivkovic J, Heier C, Mrak I, Lass A (2013) Development of small-molecule inhibitors targeting adipose triglyceride lipase. Nat Chem Biol 9:785–787. https://doi.org/10.1038/nchembio.1359

Ning LJ, He AY, Li JM, Lu DL, Jiao JG, Li LY, Li DL, Zhang ML, Chen LQ, Du ZY (2016) Mechanisms and metabolic regulation of PPARα activation in Nile tilapia (*Oreochromis niloticus*). Biochim Biophys Acta 1861:1036–1048. https://doi.org/10.1016/j.bbalip.2016.06.005

Obrowsky S, Chandak PG, Patankar JV, Povoden S, Schlager S, Kershaw EE, Bogner-Strauss JG, Hoefler G, Levak-Frank S, Kratky D (2013) Adipose triglyceride lipase is a TG hydrolase of the small intestine and regulates intestinal PPARα signaling. J Lipid Res 54:425–435. https://doi.org/10.1194/jlr.M031716

Ong KT, Mashek MT, Bu SY, Greenberg AS, Mashek DG (2011) Adipose triglyceride lipase is a major hepatic lipase that regulates triacylglycerol turnover and fatty acid signaling and partitioning. Hepatology 53:116–126. https://doi.org/10.1002/hep.24006

Parhofer KG (2015) Interaction between glucose and lipid metabolism: more than diabetic dyslipidemia. Diabetes Metab J 39:353–362. https://doi.org/10.4093/dmj.2015.39.5.353

Perry RJ, Samuel VT, Petersen KF, Shulman GI (2014) The role of hepatic lipids in hepatic insulin resistance and type 2 diabetes. Nature 510:84–91. https://doi.org/10.1038/nature13478

Peyot ML, Guay C, Latour MG, Lamontagne J, Lussier R, Pineda M, Ruderman NB, Haemmerle G, Zechner R, Joly É (2009)

Author's personal copy

Adipose triglyceride lipase is implicated in fuel-and non-fuel-stimulated insulin secretion. J Biol Chem 284:16848–16859. https://doi.org/10.1074/jbc.M109.006650

Raben DM, Baldassare JJ (2005) A new lipase in regulating lipid mobilization: hormone-sensitive lipase is not alone. Trends Endocrinol Metab 16:35–36. https://doi.org/10.1016/j.tem.2005.01.009

Rambold AS, Cohen S, Lippincott-Schwartz J (2015) Fatty acid trafficking in starved cells: regulation by lipid droplet lipolysis, autophagy, and mitochondrial fusion dynamics. Dev Cell 32:678–692. https://doi.org/10.1016/j.devcel.2015.01.029

Reid BN, Ables GP, Otlivanchik OA, Schoiswohl G, Zechner R, Blaner WS, Goldberg IJ, Schwabe RF, Chua SC, Huang LS (2008) Hepatic overexpression of hormone-sensitive lipase and adipose triglyceride lipase promotes fatty acid oxidation, stimulates direct release of free fatty acids, and ameliorates steatosis. J Biol Chem 283:13087–13099. https://doi.org/10.1074/jbc.M800533200

Reue K (2011) A thematic review series: lipid droplet storage and metabolism: from yeast to man. J Lipid Res 52:1865–1868. https://doi.org/10.1194/jlr.E020602

Rodriguez JA, Ali YB, Abdelkafi S, Mendoza LD, Leclaire J, Fotiadu F, Buono G, Carrière F, Abousalham A (2010) In vitro stereoselective hydrolysis of diacylglycerols by hormone-sensitive lipase. Biochim Biophys Acta 1801:77–83. https://doi.org/10.1016/j.bbalip.2009.09.020

Sathyanarayan A, Mashek MT, Mashek DG (2017) ATGL promotes autophagy/lipophagy via SIRT1 to control hepatic lipid droplet catabolism. Cell Rep 19:1–9. https://doi.org/10.1016/j.celrep.2017.03.026

Schoiswohl G, Stefanovic-Racic M, Menke MN, Wills RC, Surlow BA, Basantani MK, Sitnick MT, Cai L, Yazbeck CF, Stolz DB (2015) Impact of reduced ATGL-mediated adipocyte lipolysis on obesity-associated insulin resistance and inflammation in male mice. Endocrinology 156:3610–3624. https://doi.org/10.1210/en.2015-1322

Schreiber R, Xie H, Schweiger M (2019) Of mice and men: the physiological role of adipose triglyceride lipase (ATGL). Biochim Biophys Acta Mol Cell Biol Lipids 1864:880–899. https://doi.org/10.1016/j.bbalip.2018.10.008

Schulze RJ, Sathyanarayan A, Mashek DG (2017) Breaking fat: the regulation and mechanisms of lipophagy. Biochim Biophys Acta 1862:1178–1187. https://doi.org/10.1016/j.bbalip.2017.06.008

Schweiger M, Schreiber R, Haemmerle G, Lass A, Fledelius C, Jacobsen P, Tornqvist H, Zechner R, Zimmermann R (2006) Adipose triglyceride lipase and hormone-sensitive lipase are the major enzymes in adipose tissue triacylglycerol catabolism. J Biol Chem 281:40236–40241. https://doi.org/10.1074/jbc.M608048200

Schweiger M, Romauch M, Schreiber R, Grabner GF, Hütter S, Kotzbeck P, Benedikt P, Eichmann TO, Yamada S, Knittelfelder O (2017) Pharmacological inhibition of adipose triglyceride lipase corrects high-fat diet-induced insulin resistance and hepatosteatosis in mice. Nat Commun 8:14859. https://doi.org/10.1038/ncomms14859

Singh R, Cuervo AM (2012) Lipophagy: connecting autophagy and lipid metabolism. Int J Cell Biol 2012:282041–282012. https://doi.org/10.1155/2012/282041

Smirnova E, Goldberg EB, Makarova KS, Lin L, Brown WJ, Jackson CL (2006) ATGL has a key role in lipid droplet/adiposome degradation in mammalian cells. EMBO Rep 7:106–113. https://doi.org/10.1038/sj.embor.7400559

Stone DA (2003) Dietary carbohydrate utilization by fish. Rev Fish Sci 11:337–369. https://doi.org/10.1080/10641260390260884

Sun J, Ji H, Li XX, Shi XC, Du ZY, Chen LQ (2016) Lipolytic enzymes involving lipolysis in teleost: Synteny, structure, tissue distribution, and expression in grass carp (*Ctenopharyngodon idella*). Comp Biochem Physiol B Biochem Mol Biol 198:110–118. https://doi.org/10.1016/j.cbpb.2016.04.008

Turpin SM, Hoy AJ, Brown RD, Rudaz CG, Honeyman J, Matzaris M, Watt MJ (2011) Adipose triacylglycerol lipase is a major regulator of hepatic lipid metabolism but not insulin sensitivity in mice. Diabetologia 54:146–156. https://doi.org/10.1007/s00125-010-1895-5

Van Herpen NA, Schrauwen-Hinderling VB (2008) Lipid accumulation in non-adipose tissue and lipotoxicity. Physiol Behav 94:231–241. https://doi.org/10.1016/j.physbeh.2007.11.049

Wang X, Wang Y, Li Y (2013) Adipose triglyceride lipase (ATGL) clone, expression pattern, and regulation by different lipid sources and lipid levels in large yellow croaker (*Pseudosciaena crocea R.*). Mar Biotechnol 15:197–205. https://doi.org/10.1007/s10126-012-9477-9

Wang J, Han SL, Li LY, Lu DL, Limbu SM, Li DL, Zhang ML, Du ZY (2018) Lipophagy is essential for lipid metabolism in fish. Sci Bull 63:879–882. https://doi.org/10.1016/j.scib.2018.05.026

Wang J, Han SL, Lu DL, Li LY, Limbu SM, Li DL, Zhang ML, Du ZY (2019) Inhibited lipophagy suppresses lipid metabolism in zebrafish liver cells. Front Physiol 10:1077. https://doi.org/10.3389/fphys.2019.01077

Williams MB, Watts SA (2019) Current basis and future directions of zebrafish nutrigenomics. Genes Nutr 14:34. https://doi.org/10.1186/s12263-019-0658-2

Wu JW, Wang SP, Alvarez F, Casavant S, Gauthier N, Abed L, Soni KG, Yang G, Mitchell GA (2011) Deficiency of liver adipose triglyceride lipase in mice causes progressive hepatic steatosis. Hepatology 54:122–132. https://doi.org/10.1002/hep.24338

Wu JW, Wang SP, Casavant S, Moreau A, Yang GS, Mitchell GA (2012) Fasting energy homeostasis in mice with adipose deficiency of desnutrin/adipose triglyceride lipase. Endocrinology 153:2198–2207. https://doi.org/10.1210/en.2011-1518

Xia B, Cai GH, Yang H, Wang SP, Mitchell GA, Wu JW (2017) Adipose tissue deficiency of hormone-sensitive lipase causes fatty liver in mice. PLoS Genet 13:e1007110. https://doi.org/10.1371/journal.pgen.1007110

Xie P, Guo F, Ma Y, Zhu H, Wang F, Xue B, Shi H, Yang J, Yu L (2014) Intestinal Cgi-58 deficiency reduces postprandial lipid absorption. PLoS One 9:e91652. https://doi.org/10.1371/journal.pone.0091652

Yan J, Liao K, Wang T, Mai K, Xu W, Ai Q (2015) Dietary lipid levels influence lipid deposition in the liver of large yellow croaker (*Larimichthys crocea*) by regulating lipoprotein receptors, fatty acid uptake and triacylglycerol synthesis and

Author's personal copy

catabolism at the transcriptional level. PLoS One 10: e0129937. https://doi.org/10.1371/journal.pone.0129937

Yang L, Li P, Fu S, Calay ES, Hotamisligil GS (2010) Defective hepatic autophagy in obesity promotes ER stress and causes insulin resistance. Cell Metab 11:467–478. https://doi.org/10.1016/j.cmet.2010.04.005

Yang BY, Zhai G, Gong YL, Su JZ, Peng XY, Shang GH, Han D, Jin JY, Liu HK, Du ZY, Yin Z, Xie SQ (2017) Different physiological roles of insulin receptors in mediating nutrient metabolism in zebrafish. Am J Physiol Endocrinol Metab 315:E38–E51. https://doi.org/10.1152/ajpendo.00227.2017

Zechner R, Zimmermann R, Eichmann TO, Kohlwein SD, Haemmerle G, Lass A, Madeo F (2012) FAT SIGNALS-lipases and lipolysis in lipid metabolism and signaling. Cell Metab 15:279–291. https://doi.org/10.1016/j.cmet.2011.12.018

Zechner R, Madeo F, Kratky D (2017) Cytosolic lipolysis and lipophagy: two sides of the same coin. Nat Rev Mol Cell Biol 18:671–684. https://doi.org/10.1038/nrm.2017.76

Zhang Z, Yao Z, Chen Y, Qian L, Jiang S, Zhou J, Shao J, Chen A, Zhang F, Zheng S (2018) Lipophagy and liver disease: new perspectives to better understanding and therapy. Biomed Pharmacother 97:339–348. https://doi.org/10.1016/j.biopha.2017.07.168

Zhang X, Zhang CC, Yang H, Soni KG, Wang SP, Mitchell GA, Wu JW (2019) An epistatic interaction between Pnpla2 and Lipe reveals new pathways of adipose tissue lipolysis. Cells 8:395. https://doi.org/10.3390/cells8050395

Zhao T, Wu K, Hogstrand C, Xu YH, Chen GH, Wei CC, Luo Z (2019) Lipophagy mediated carbohydrate-induced changes of lipid metabolism via oxidative stress, endoplasmic reticulum (ER) stress and ChREBP/PPARγ pathways. Cell Mol Life Sci 77:1987–2003. https://doi.org/10.1007/s00018-019-03263-6

Zimmermann R, Strauss JG, Haemmerle G, Schoiswohl G, Birner-Gruenberger R, Riederer M, Lass A, Neuberger G, Eisenhaber F, Hermetter A (2004) Fat mobilization in adipose tissue is promoted by adipose triglyceride lipase. Science 306:1383–1386. https://doi.org/10.1126/science.1100747

Publisher's note Springer Nature remains neutral with regard to jurisdictional claims in published maps and institutional affiliations.